Synthesis and material characterization of amorphous and crystalline (α-) Al_2O_3 *via* aerosol assisted chemical vapour deposition.

Sapna D. Ponja[a], Ivan P. Parkin[a] and Claire J. Carmalt[a]*

*Corresponding author

[a]Materials Chemistry Centre, Department of Chemistry, University College London, 20 Gordon Street, London WC1H 0AJ, UK

Fax: (+44) 20-7679-7463

E-mail: c.j.carmalt@ucl.ac.uk

Abstract

The facile synthesis of Al_2O_3 in the amorphous and corundum phase on both glass and quartz substrates are reported. Synthesis was carried out *via* aerosol assisted chemical vapour deposition using $Al(acac)_3$ and methanol. The films were analyzed using XRD, SEM, UV-vis spectroscopy and XPS. The coatings were highly crystalline (when annealed) with low carbon contamination levels and a relatively featureless morphology that gave rise to ultra high transparency in the UV, visible and near IR portions of the electromagnetic spectrum.

Introduction

Various metastable crystalline phases of alumina exist, with either face centred cubic (fcc) or hexagonal close packed (hcp) structures.[1] The corundum phase (α-alumina), formed at temperatures above 1000 ^{o}C, is the most thermodynamically stable and exhibits hcp arrangement in which aluminium ions occupy two-thirds of the octahedral interstices.[2-4] The outstanding stability, along with high transparency due to a band gap of 8.7 eV, lends itself to a range of applications including the protective coatings of materials such as metals, high temperature insulation for microelectronic devices including dielectrics and diffusion barrier coatings.[1, 3, 5-6] Structural specificity also widens the applications of alumina films, for example, the greater surface area, attributed to the fcc arrangement, allowing them to be more effective as catalysts and catalytic supports.[1]

Alumina films have been deposited using several established methods employing mostly organic based precursors.[2, 6] The problem faced in manufacturing alumina films is eliminating carbon contamination during low temperature depositions.[3, 5] A variety of precursors have been used to deposit alumina films, including aluminium chloride[4] and alkoxides such as aluminium tri-isopropoxide.[3, 7] Both have disadvantages in that the former produces hydrogen chloride gas and the alkoxides are highly moisture sensitive as well as readily forming oligomers hence reducing their volatility.[5] Aluminium acetylacetonate has been used as an alternative precursor since it has the advantages of being relatively less toxic, easier to handle and high volatility at high temperatures.[8]

In this paper we describe the deposition of alumina films using aluminium acetylacetonate *via* aerosol-assisted chemical vapour deposition (AACVD). AACVD is a simple, scalable, solution based method that produces high quality films and can exploit a wide range of precursors without the need for them to be volatile at high temperatures.[9]

Experimental

Depositions were carried out under nitrogen (99.99% from BOC). All chemicals were obtained from Sigma Aldrich and used as received. The precursor aluminium acetylacetonate was dissolved in methanol (0.20 g in 20 ml) and placed in a glass bubbler and an aerosol mist was created at room temperature using a piezoelectric device. The alumina films were deposited *via* AACVD onto SiO_2 barrier coated (50 nm) float-glass (Pilkington NSG Ltd) or quartz (Chemglass Life Sciences) at 500 ^oC under N_2 carrier gas at a flow rate of 1.0 L min^{-1}. The glass substrate was washed prior to use with water and detergent, propan-2-ol and propanone and air dried.

The depositions were carried out in a CVD rig constructed in-house.[10] The rig consisted of an open ended quartz tube caped at both ends with stainless steel plates, the inlet and outlet plates. The steel plates support the upper plate which was placed about 5 mm above the glass bottom plate. The glass substrate was heated in the rig on top of a graphite heating block containing a Whatman cartridge heater. The substrate temperature was controlled and monitored using a Pt-Rh thermocouple. The inlet plate was attached to a brass baffle which directs the flow of the aerosol in the carrier gas into the chamber and together with the top plate they ensure a laminar gas flow. Any unreacted chemicals and reaction by-products left *via* the exhaust in the outlet end plate.

The film deposited on quartz was annealed at 1100 ^oC in air overnight.

Analysis of the films

X-ray photoelectron spectroscopy (XPS) analysis were performed using a JEOL JSM-6301F field-emission instrument with acceleration voltage of 5 kV.

Scanning electron microscopy (SEM) was performed on a JEOL JSM-6700F instrument using an accelerating voltage of 5 kV.

X-ray diffraction (XRD) was carried out with a Bruker D8 GAADS powder X-ray diffractometer with monochromated $Cu_{K\alpha1}$ (1.54056 Å) and $Cu_{K\alpha2}$ (1.54439 Å) radiation with an intensity ratio of 2:1, a voltage of 40 kV and current of 40 mA. The X-ray incident angle was 0.5° and the angular range of the patterns collected was $10° < 2\theta < 66°$ with a step size of 0.05° counted at 4 s/step.

UV/Vis/near-IR transmittance and reflectance spectra were produced from data obtained from a Perkin–Elmer Lambda 950 spectrometer using air as the background and recorded between 320–2500 nm.

Results and Discussion

Thin films of amorphous Al_2O_3 were deposited on glass and quartz *via* the AACVD reaction of $Al(acac)_3$ and methanol at 500 ^oC, carried over using a N_2 flow of 1 L min^{-1}. The as deposited films on quartz were subsequently annealed under air overnight at 1100 ^oC to obtain the corundum phase (α-Al_2O_3). Both the as deposited and annealed films on glass and quartz were highly transparent in the visible and well adhered to the substrate, passing the Scotch^{TM} tape test.

Figure 1 shows the powder X-ray diffraction (XRD) patterns for the as deposited and annealed films. The as deposited film shows the typical pattern with no diffraction peaks that is expected for an amorphous substance. However, the air annealed film on quartz showed well defined diffraction peaks matching to the thermodynamically stable corundum phase with hexagonal crystal symmetry that is normally expect for Al_2O_3 above 1000 ^oC. Peaks were observed at 25.6^o (012), 35.1^o (104), 37.8^o (110), 43.5^o (113), 52.6^o (024), 57.6^o (116) and 61.3^o (018) matching well with the standard.

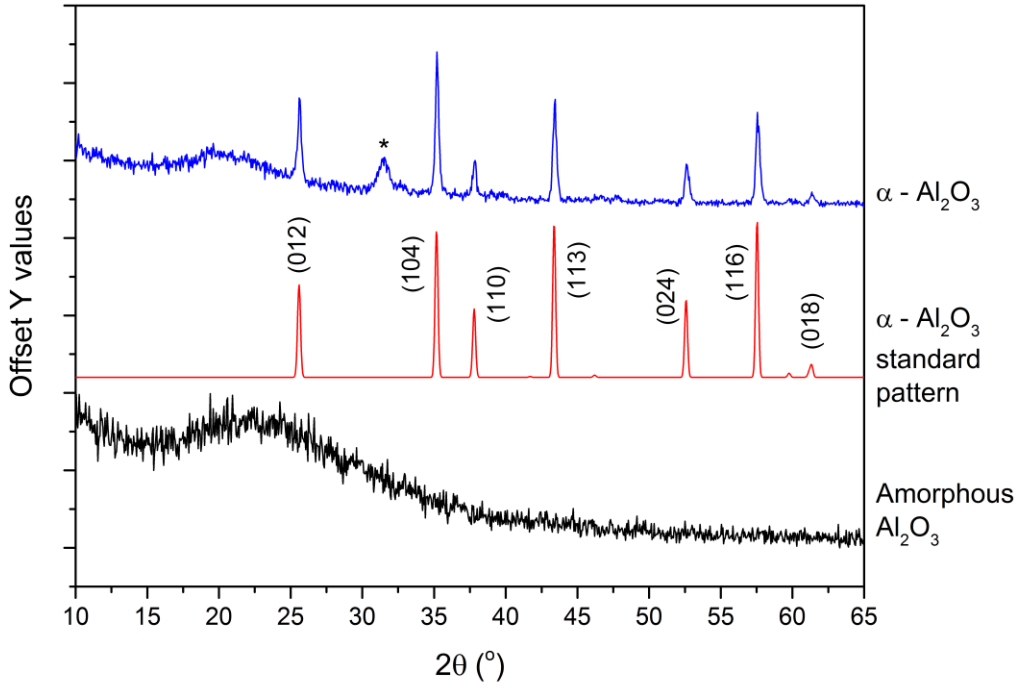

Figure 1: The PXRD patterns of the a) as deposited amorphous Al_2O_3 film on glass and b) the annealed α-Al_2O_3 on quartz. * Indicates reflection due to the quartz substrate.

The morphology of the films was studied using scanning electron microscopy (SEM) and is shown in Figure 2. The amorphous film surface structure consists of densely

packed spheres between 300 and 1000 nm in diameter. Upon annealing the morphology of the film changes dramatically, becoming markedly flatter and featureless. This is most likely due to grain growth initiated by the high temperature. The annealing process also imparted pinholes into the α-Al_2O_3 film.

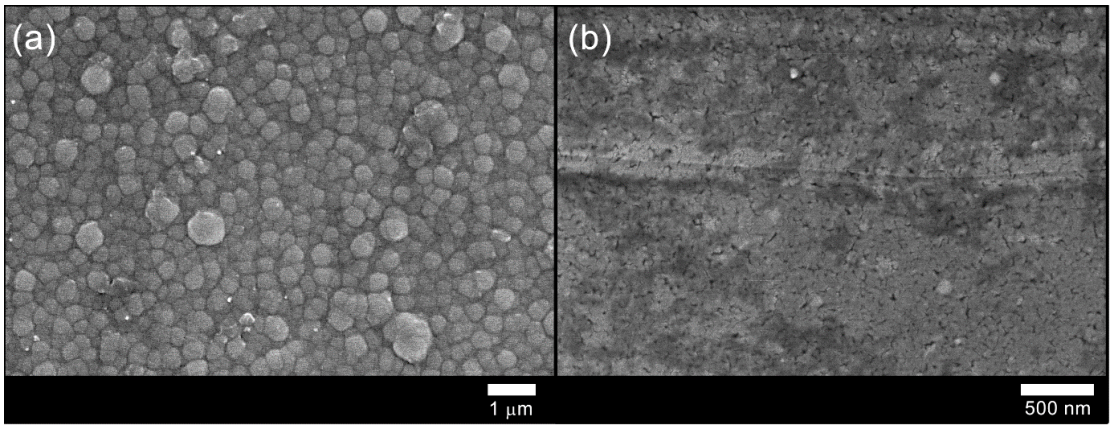

Figure 2: SEM images of a) as deposited amorphous Al_2O_3 film on glass and b) the annealed α-Al_2O_3 on quartz.

The transmission and reflectance properties of the films were investigated using visible/near IR spectrometry (Fig. 3). The films showed a high transparency of over 85% at 550 nm in air. The transparency of the annealed film on quartz remained relatively constant over the wavelength range investigated whereas the transparency of the amorphous film showed only slightly lower transparency in the visible region. Reflectance for both films remained consistently low (ca. 10%) across all wavelengths measured. The high transparency and low reflectance of the as deposited amorphous film is attributed to the low carbon contamination levels achieved through the AACVD process. The higher transparency of the crystalline α-Al_2O_3 was due to the annealing step that was able to oxidize and remove most of the residual carbon contamination from the growth process

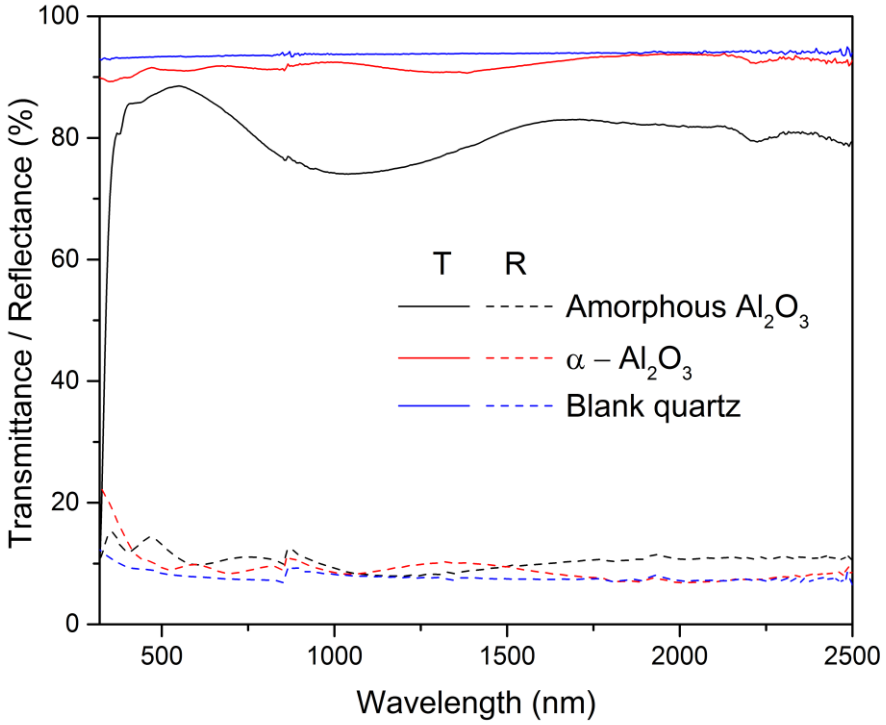

Figure 3: UV –Vis spectra encompassing the UV, visible and near IR wavelengths for the amorphous Al_2O_3 on glass and α-Al_2O_3 on quartz.

The carbon levels on the surface and in the bulk of the films, determined using X-ray photoelectron spectroscopy (XPS), showed that contamination was predominately on the surface. Upon Ar^+ ion etching for 400 seconds the C levels reduce to >5 at.% relative to Al and this remains consistent even after 1200 seconds.

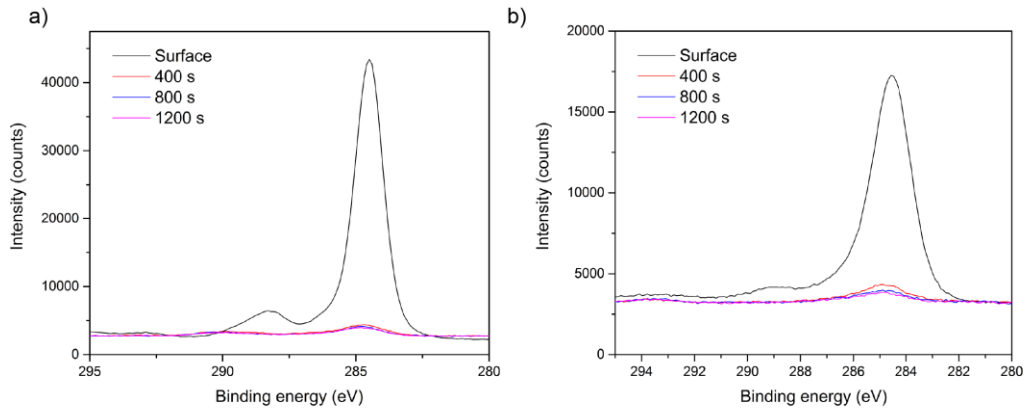

Figure 4: XPS spectra showing the change in carbon contamination levels with sputtering time.

XPS was also used to determine the oxidation state of Al on the surface (Figure 4a and b). XPS allows the differentiation between Al(0) and its compounds with the difference in binding energy being about 2 eV and the metal peak width narrower than for the materials. The peaks observed in the present study were 73.8 eV for both glass and quartz (Figure 4a and b). These values correspond to those typical of aluminum compounds, in particular oxides and hydroxides.[5-6, 11] The expectation of modelling the Al 2p peak would be a doublet however the separation of Al $2p_{1/2}$ and Al $2p_{3/2}$ is not significant to do so. Hence, the Al 2p peak is commonly modelled as a single peak.[6, 11-12] The binding energies for the oxides and hydroxides of Al are similar within the range 74-75 eV making it impossible to distinguish between the different compounds.[6, 11]

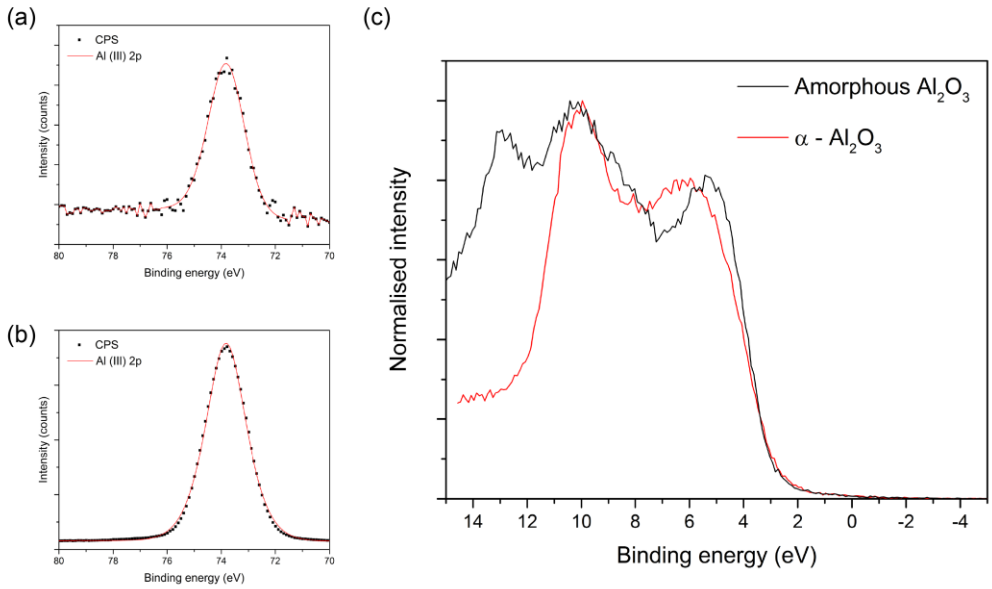

Figure 5: a) Core level and b) valence band XPS spectra for the amorphous Al_2O_3 film on glass and α-Al_2O_3 quartz.

The valence band of Al_2O_3, like that of SiO_2, is known to be composed of two subbands, the lower subband (at around 20 eV) and the upper subband (between 0 and 12 eV).[13-14] Here we will focus on the upper subband that encompasses the valence band maxima (VBM) (Figure 5c). The position of the VBM with respect to the Fermi level (set to 0 eV) was determined through the simple extrapolation of the leading edge of the lowest energy band to be 2.9 eV and 2.7 eV for the amorphous and α-Al_2O_3 films. This matches

well with literature reports.[13-14] The upper subband of both films is composed of intermixed O 2p and Al 3s, 3p and 3d orbitals.[13] The fine structure observed in the upper subband consists of a peak around 5.8 and 10 eV for both films. The peak around 5.8 eV is known to be made up of antibonding 2pπ orbitals of O while the peak around 10 eV is derived from the bonding 2pσ orbitals of O that are mixed with the 3s, 3p and 3d orbitals of Al.[13 14] The bonding O 2pσ orbitals mixed with the Al 3s, 3p and 3d are said to be found between these two features.[13] The slight variation in the band positions between the amorphous and crystalline films was due to the sensitivity of the valence band positions to the crystal structure.

The alumina films showed no change in the water contact angle after the annealing process. This was despite there being a marked change in the morphology of the films upon heat treatment.

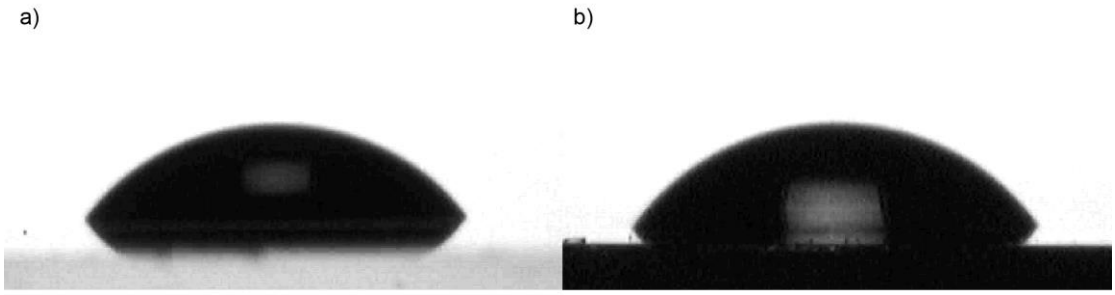

Figure 6: The water contact angle on the surface of the amorphous and α-Al_2O_3 films was 55º.

Conclusion

In conclusion we report the first synthesis via AACVD from $Al(acac)_3$ and methanol of low carbon contaminated, highly transparent amorphous Al_2O_3 thin films. Films deposited on quartz were also annealed in air at 1100 ºC to obtain the corundum crystal phase. SEM images showed the films to be relatively featureless and flat even after the annealing step, thus making them ideal dielectric and optical coatings. XPS analysis of the films showed relative low carbon levels in the bulk in both the pre and post annealed films.

References

1. Dhonge, B. P.; Mathews, T.; Sundari, S. T.; Kamruddin, M.; Dash, S.; Tyagi, A. K., Combustion chemical vapour deposition of Al2O3 films: Effect of temperature on structure, morphology and adhesion. *Surface and Coatings Technology* **2010,** *205* (7), 1838-1842.
2. Pradhan, S. K.; Reucroft, P. J.; Ko, Y., Crystallinity of Al2O3 films deposited by metalorganic chemical vapor deposition. *Surface and Coatings Technology* **2004,** *176* (3), 382-384.
3. Blittersdorf, S.; Bahlawane, N.; Kohse-Höinghaus, K.; Atakan, B.; Müller, J., CVD of Al2O3 Thin Films Using Aluminum Tri-isopropoxide. *Chemical Vapor Deposition* **2003,** *9* (4), 194-198.
4. Fredriksson, E.; Carlsson, J.-O., Factors influencing the κ -Al2O3 $\rightarrow$ α -Al2O3 phase transformation during CVD growth. *Surface and Coatings Technology* **1993,** *56* (2), 165-177.
5. Knapp, C. E.; Marchand, P.; Dyer, C.; Parkin, I. P.; Carmalt, C. J., Synthesis and characterisation of novel aluminium and gallium precursors for chemical vapour deposition. *New Journal of Chemistry* **2015,** *39* (8), 6585-6592.
6. Etchepare, P.-L.; Baggetto, L.; Vergnes, H.; Samélor, D.; Sadowski, D.; Caussat, B.; Vahlas, C., Process-structure-properties relationship in direct liquid injection chemical vapor deposition of amorphous alumina from aluminum tri-isopropoxide. *physica status solidi (c)* **2015,** *12* (7), 944-952.
7. Etchepare, P. L.; Vergnes, H.; Samélor, D.; Sadowski, D.; Caussat, B.; Vahlas, C., Modeling a MOCVD process to apply alumina films on the inner surface of bottles. *Surface and Coatings Technology* **2015,** *275*, 167-175.
8. Kim, J. S.; Marzouk, H. A.; Reucroft, P. J.; Robertson, J. D.; Hamrin, C. E., Effect of water vapor on the growth of aluminum oxide films by low pressure chemical vapor deposition. *Thin Solid Films* **1993,** *230* (2), 156-159.
9. Knapp, C. E.; Carmalt, C. J., Solution based CVD of main group materials. *Chemical Society Reviews* **2016,** *45* (4), 1036-1064.
10. Ponja, S. D.; Sathasivam, S.; Parkin, I. P.; Carmalt, C. J., Transparent conductive aluminium and fluorine co-doped zinc oxide films via aerosol assisted chemical vapour deposition. *RSC Advances* **2014,** *4* (91), 49723-49728.
11. Sherwood, P. M. A., Introduction to Studies of Aluminum and its Compounds by XPS. *Surface Science Spectra* **1998,** *5* (1), 1-3.
12. Duan, X.; Tran, N. H.; Roberts, N. K.; Lamb, R. N., Single-source chemical vapor deposition of clean oriented Al2O3 thin films. *Thin Solid Films* **2009,** *517* (24), 6726-6730.
13. Filatova, E. O.; Konashuk, A. S., Interpretation of the Changing the Band Gap of Al2O3 Depending on Its Crystalline Form: Connection with Different Local Symmetries. *The Journal of Physical Chemistry C* **2015,** *119* (35), 20755-20761.
14. Perevalov, T. V.; Shaposhnikov, A. V.; Gritsenko, V. A.; Wong, H.; Han, J. H.; Kim, C. W., Electronic structure of α-Al2O3: Ab initio simulations and comparison with experiment. *JETP Letters* **2007,** *85* (3), 165-168.